

Supplemental Information

In-Materio Reservoir Working at Low Frequencies in a Ag₂S-island Network

Motoharu Nakajima,^a Kazuki Minegishi,^a Yosuke Shimizu,^a Yuki Usami,^{b,c} Hiroyumi Tanaka,^{b,c} and Tsuyoshi Hasegawa^{*a}

^aDepartment of Pure and Applied Physics, Graduate School of Advanced Science and Engineering, Waseda University, 3-4-1 Okubo, Shinjuku-ku, Tokyo 169-8555, Japan

^bDepartment of Human Intelligence Systems, Graduate School of Life Science and Systems Engineering, Kyushu Institute of Technology, 2-4 Hibikino, Wakamatsu, Kitakyushu 808-0196, Japan

^cResearch Center for Neuromorphic AI Hardware, Kyushu Institute of Technology

1. Characteristics of the Ag₂S island network of 30 μm in diameter

Similar to the 1 μm-Ag₂S island network, a 30 μm-Ag₂S island network showed the dependence of ΔR on the frequency and amplitude of inputs. Figure S1 shows the change in ΔR as a function of input frequency. As can be seen, ΔR of the 30 μm-network, indicated by red open triangles, shows almost the same characteristics with ΔR of the 1 μm-network, indicated by blue open triangles. Figure S2 shows the change in ΔR of the 30 μm-network as a function of the input amplitude, which also shows the similar characteristic with that of the 1 μm-network shown in Fig. 4b. These results suggest the expansion capability of a Ag₂S island network as a reservoir.

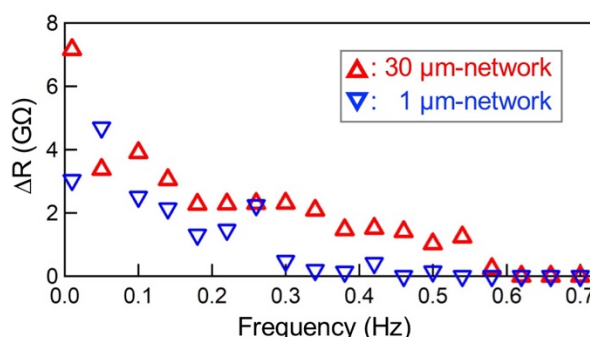


Figure S1. Change in ΔR as a function of frequency.

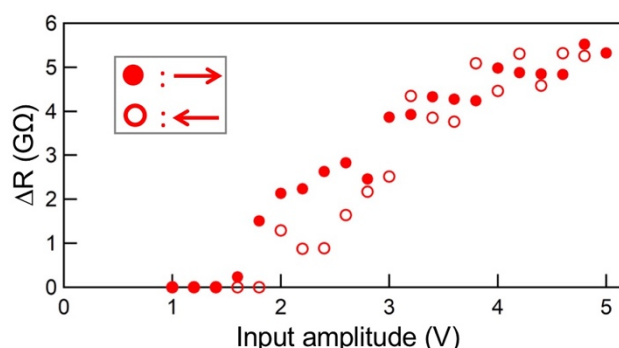


Figure S2. Change in ΔR as a function of input amplitude.

2. Logic operations using the Ag₂S island network of 30 μm in diameter with sixteen electrodes

2.1 Logic operations at 0.2 Hz

Fourteen outputs, $O_1 - O_{14}$ that are shown in Fig. 6c, are shown in each panel of Fig. S3. Optimized weights, $w_1 - w_{14}$, and bias, w_0 , used for each logic operation are listed in Table. S1.

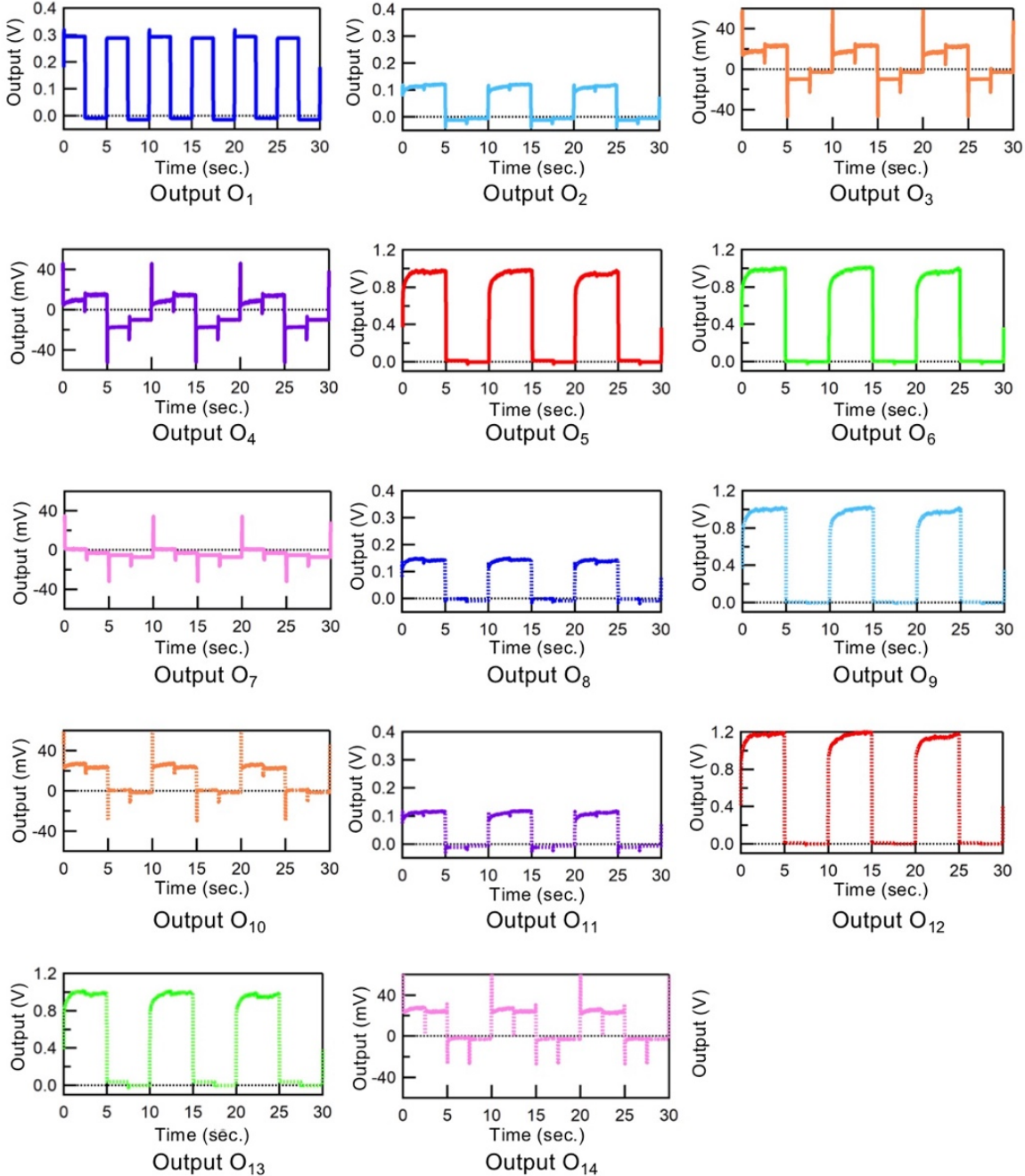


Figure S3. Fourteen outputs used in the synthesis of the six logic operations shown in Fig. 7.

Table S1. Weights and a bias used for the logic operations shown in Fig. 7.

	AND	NAND	OR	NOR	XOR	XNOR
w_1	14.27271444	-14.27271444	-16.2438729	16.2438729	-30.5165873	30.5165873
w_2	32.09701703	-32.09701703	-38.9124885	38.9124885	-71.00950554	71.00950554
w_3	-166.6766858	166.6766858	107.122603	-107.122603	273.79928876	-273.79928876
w_4	-74.90677803	74.90677803	69.8550458	-69.8550458	144.76182379	-144.76182379
w_5	132.00542533	-132.00542533	-109.303097	109.303097	-241.30852252	241.30852252
w_6	-24.41800565	24.41800565	24.0349571	-24.0349571	48.4529628	-48.4529628
w_7	-19.29269241	19.29269241	7.29002473	-7.29002473	26.58271714	-26.58271714
w_8	0.95773778	-0.95773778	-18.2128497	18.2128497	-19.17058752	19.17058752
w_9	8.3724351	-8.3724351	-71.9385144	71.9385144	-80.31094952	80.31094952
w_{10}	193.58686444	-193.58686444	-106.122638	106.122638	-299.70950214	299.70950214
w_{11}	73.36477611	-73.36477611	-49.1073162	49.1073162	-122.47209235	122.47209235
w_{12}	71.78217991	-71.78217991	-61.8458743	61.8458743	-133.62805425	133.62805425
w_{13}	-213.02184081	213.02184081	245.487179	-245.487179	458.50902014	-458.50902014
w_{14}	41.57756917	-41.57756917	-50.8160186	50.8160186	-92.39358777	92.39358777
w_0	-0.50957948	0.991970	0.183284762	1.000170	0.69286424	0.995001

2.2 Logic operations at 2 Hz

Logic operations used higher frequency (2Hz) are shown in Fig. S4. Two inputs and fourteen outputs are shown in Fig. S5. Weights and a bias used for the synthesis are listed in Table S2.

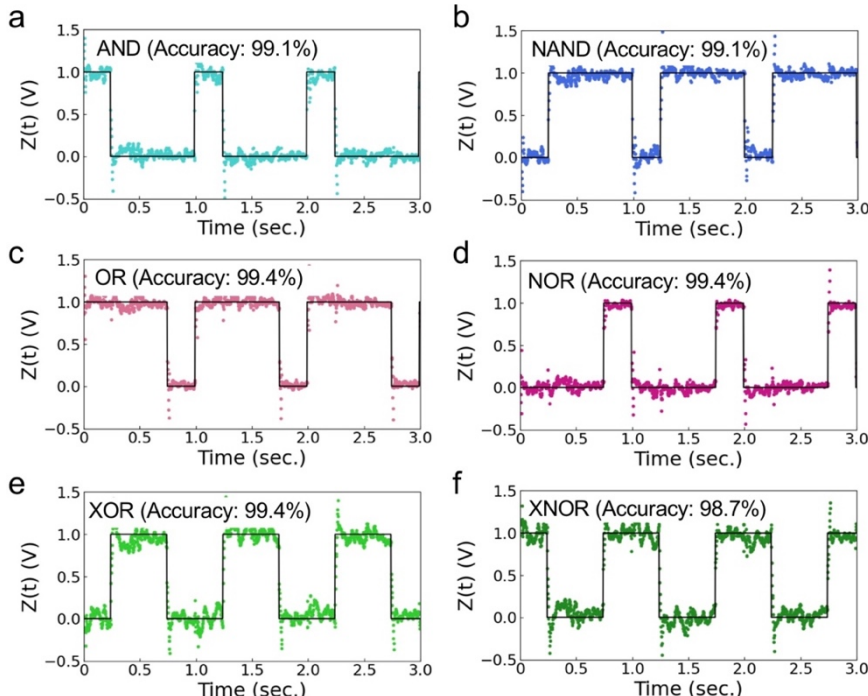


Figure S4. Logic operations using inputs of 2 Hz. Synthesized curves are shown by colored curve in each panel. The target in each logic operation is shown by the black solid lines.

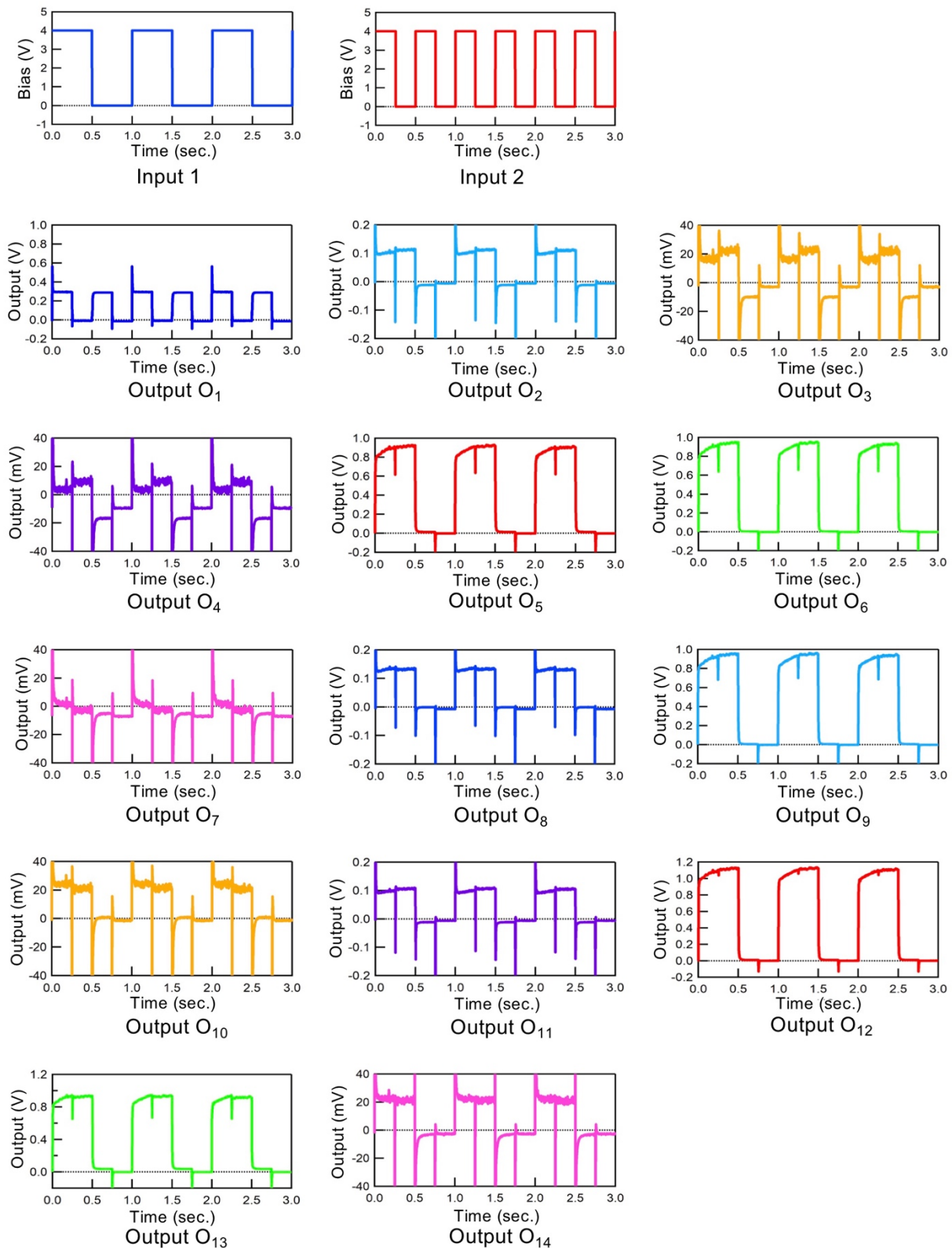


Figure S5. Inputs of 1Hz and 2 Hz square waves and fourteen outputs used for the six logic operations shown in Fig. S4.

Table S2. Weights and a bias used for the logic operations shown in Fig. S4.

	AND	NAND	OR	NOR	XOR	XNOR
w_1	14.53360267	-14.53360267	-13.42211438	13.42211438	-31.93642764	31.93642764
w_2	-76.19190972	76.19190972	41.7576958	-41.7576958	110.15997087	-110.15997087
w_3	27.08537777	-27.08537777	5.75201011	-5.75201011	-35.4658381	35.4658381
w_4	92.35950635	-92.35950635	-83.51453882	83.51453882	-195.62746705	195.62746705
w_5	223.14605355	-223.14605355	-207.9388385	207.9388385	-422.03126604	422.03126604
w_6	-14.81471796	14.81471796	23.33365079	-23.33365079	20.19565788	-20.19565788
w_7	110.88073398	-110.88073398	-58.49396508	58.49396508	-166.4526384	166.4526384
w_8	99.45836774	-99.45836774	26.13528055	-26.13528055	-32.75687786	32.75687786
w_9	-74.1576281	74.1576281	46.56313875	-46.56313875	127.36790425	-127.36790425
w_{10}	-275.55498574	275.55498574	142.32506532	-142.32506532	484.62814437	-484.62814437
w_{11}	6.68380815	-6.68380815	-34.31699715	34.31699715	-91.4383641	91.4383641
w_{12}	43.27078136	-43.27078136	-44.7379075	44.7379075	-89.96982525	89.96982525
w_{13}	-184.09791706	184.09791706	182.20522359	-182.20522359	371.34652432	-371.34652432
w_{14}	29.8768278	-29.8768278	-26.70769163	26.70769163	57.78318296	-57.78318296
w_0	1.63799742	-0.63799742	-0.71933416	1.71933416	-2.60276472	3.60276472